Available online at www.sciencedirect.com
SCIENCE DIRECT
Biochimica et Biophysica Acta 1713 (2005) 15 – 28
BIOCHIMICA ET BIOPHYSICA ACTA
BBA
http://www.elsevier.com/locate/bba

The structure of DNA–DOPC aggregates formed in presence of calcium and magnesium ions: A small-angle synchrotron X-ray diffraction study ☆

Daniela Uhríková[a,*], Mária Hanulová[b], Sérgio S. Funari[b], Raylja S. Khusainova[c], František Šeršeň[a], Pavol Balgavý[a]

[a]Department of Physical Chemistry of Drugs, Faculty of Pharmacy, Comenius University, 832 32 Bratislava, Slovakia
[b]Max-Planck-Institute of Colloids and Interfaces, c/o HASYLAB, DESY, D-22603 Hamburg, Germany
[c]Institute of Theoretical and Experimental Biophysics, Russian Academy of Sciences, Pushchino, Moscow Region, 142292, Russia

Received 12 November 2004; received in revised form 30 April 2005; accepted 12 May 2005
Available online 1 June 2005

Abstract

The structure of aggregates formed due to DNA interaction with dioleoylphosphatidylcholine (DOPC) vesicles in presence of Ca^{2+} and Mg^{2+} cations was investigated using synchrotron small-angle X-ray diffraction. For DOPC/DNA=1:1 mol/base and in the range of concentration of the cation^{2+} 0–76.5 mM, the diffractograms show the coexistence of two lamellar phases: L^x phase with repeat distance d_{Lx} ~8.26–7.39 nm identified as a phase where the DNA strands are intercalated in water layers between adjacent lipid bilayers, and L_{DOPC} phase with repeat distance d_{DOPC} ~6.45–5.65 nm identified as a phase of partially dehydrated DOPC bilayers without any divalent cations and DNA strands. The coexistence of these phases was investigated as a function of DOPC/DNA molar ratio, length of DNA fragments and temperature. If the amount of lipid increases, the fraction of partially dehydrated L_{DOPC} phase is limited, depends on the portion of DNA in the sample and also on the length of DNA fragments. Thermal behaviour of DOPC+DNA+Ca^{2+} aggregates was investigated in the range 20–80 °C. The transversal thermal expansivities of both phases were evaluated.

Keywords: DNA; Dioleoylphosphatidylcholine; Ca^{2+}; Mg^{2+}; Cationic vesicles; Small-angle X-ray diffraction

1. Introduction

It became evident recently that, in order to construct efficient liposomal genetic delivery systems, it is necessary to understand the mechanism of the formation of complexes of DNA and cationic vesicles. Essential requisites to get effective transfection vectors are the following: they must bind DNA sufficiently strongly to reach rapidly target cells and release DNA inside them. Moreover, they must be non-toxic, non-immunogenic and biodegradable. The first key step in the whole process is the compaction of the extended, high-molecular, negatively charged DNA into a dense neutral (or positively charged) particle small enough to be taken up by the cell [1–3]. Neutralization of more than 90% of the negative charges of DNA by cationic vesicles results in the condensation of DNA in structures of different morphology. Three types of condensed organized cationic surfactant–lipid–DNA microstructures are identified: (i) spaghetti-like structures in which DNA is covered by a cylindrical lipid bilayer [4], (ii) honeycomb-like condensed columnar inverted hexagonal phase with linear DNA molecules surrounded by lipid monolayers forming inverted cylindrical micelles arranged on a hexagonal lattice [5], (iii) sandwich-like with DNA monolayers intercalated between lipid bilayers (condensed lamellar phase) [6]. The positive surface charge of cationic vesicles can be created by intercalation of cationic surfactant molecules [7–9] into the neutral lipid bilayer, or by addition of small metal cations [10–13].

☆ Dedicated to Prof. Dr. Martin Bútora, PhD. on the occasion of his 60th birthday.

* Corresponding author. Tel.: +421 2 50117 289; fax: +421 2 50117 100.
E-mail address: daniela.uhrikova@fpharm.uniba.sk (D. Uhríková).

0005-2736/$ - see front matter © 2005 Elsevier B.V. All rights reserved.
doi:10.1016/j.bbamem.2005.05.006

Neutral phospholipid bilayers in presence of small metal cations (Ca^{2+}, Mg^{2+}, etc.) spontaneously form vesicles with a positive surface charge [14–16]. The formation of large light scattering aggregates due to the interaction of polynucleotides with phosphatidylcholine vesicles in presence of Mg^{2+} ions was documented more than two decades ago [10,17]. Earlier microcalorimetric and ESR studies performed in our laboratory indicated the formation of a new phase due the interaction of DNA with multilamellar and unilamellar dipalmitoylphosphatidylcholine (DPPC) vesicles in presence of Mg^{2+} ions. It was observed that the temperature of the phase transition gel–liquid crystal was higher than that of pure DPPC [11,18,19]. Khusainova et al. [20] have found that the main transition temperature of DNA+DPPC+Ca^{2+} aggregates depends on the molar ratio DPPC/DNA. The morphology of the aggregates was investigated using freeze fracture electron micrographs [12,21,22]. Small-angle X-ray diffraction experiments have shown the regular organization of DNA+neutral lipid+divalent cations aggregates and X-ray diffractograms indicated two possible structures of aggregates: The sandwich structure was observed in our previous work [13] in the DNA/DPPC/Mg^{2+}=1:1:5 base/mol/mol aggregate. In the temperature range 20–60 °C, we measured the DPPC repeat distance d_{DPPC} ~8.00–7.58 nm and the interhelical DNA distance d_{DNA} ~6.35–6.02 nm. For DPPC/DNA=8:1 mol/base aggregates formed in presence of 1–100 mM $CaCl_2$ [23,24], it was observed the coexistence of two lamellar phases: one with DNA strands intercalated in the water layer between lipid bilayers with a repeat distance ~8.0–7.4 nm (sandwich structure), and another with a repeat distance ~6.6–5.6 nm, identified as a phase formed only by lipids bilayers. The coexistence of two lamellar phases in the structure of DNA+DOPC+Mn^{2+} aggregates was reported by Francescangeli et al. [25] as well. Koltover et al. [26] discovered the ability of divalent cations to induce a sharp condensation of DNA when the strands are trapped between cationic lipid bilayers. These experimental results indicate the ability of divalent cations to compact DNA into structures with morphologies similar to those observed for DNA–lipid–cationic surfactant aggregates. The ability of these "metallonucleoliposome" aggregates to serve as vehicles for gene delivery to mammalian cells in vitro as well as in vivo was demonstrated by the group of Zhdanov [27–29].

In the present paper, we study the structure of aggregates due to the interaction of DNA with DOPC vesicles in presence of the divalent cations Ca^{2+} and Mg^{2+} using synchrotron small-angle X-ray diffraction. Diffractograms of aggregates show the coexistence of two lamellar phases. We intend to clarify the structural organization of these phases by changing the molar ratios of components and the length of DNA fragments in the aggregates. We investigate the structural parameters of the two observed phases when the aggregates are formed in solutions of metal cations in the concentration range 0–76.5 mM, at DNA/DOPC=1:1 base/mol, and their thermal behaviour in the range 20–80 °C. The analysis of the changes of the width of Bragg diffraction peaks indicates that ~20 mM $CaCl_2$ provide an optimal binding between the DNA polyanion and DOPC bilayers in DNA/DOPC=1:1 base/mol aggregates. A set of samples prepared with different lengths of DNA fragments in 20 mM $CaCl_2$ indicates an effect of these lengths on the volume fraction of each phase. The effects due to the amount of lipid were followed by changing the molar ratio DOPC/DNA $\leq$ 10:1 for aggregates prepared in 20 mM $CaCl_2$.

2. Materials and methods

2.1. Sample preparation

Highly polymerized calf thymus DNA (Sigma Chemicals Co., USA) was dissolved in 0.5 mM HEPES buffer, pH ~7, at concentration 2 mg/ml. The 8-ml volume of this solution was sonicated under nitrogen and in an ice bath using a 20-kHz titanium probe-type sonicator (Chirana, Piešťany, Slovakia) in 60 s pulses and 120 s delay. After 200 s of sonication time, 3 ml of solution was taken away and the rest of sample was sonicated up to 20 min. The procedure was repeated 4 times and the same volumes of solutions were taken away after 400, 600, 800 and 1000 s of sonication time in order to obtain fragments of DNA with different lengths. The last volume of the DNA solution was sonicated for 60 min. The portions of DNA sonicated 20 min were mixed together and used for the preparation of two sets of samples (see below). The purity and nativity of DNA after sonication were checked by measuring the absorbance A_λ at λ=260 and 280 nm. We have obtained A_{260}/A_{280}=1.8 and a change of 31% of the value of A_{260} before and after DNA denaturation.

The length of short DNA fragments was determined by electrophoretic mobility using the 3.5% polyacrylamide gel which gives an effective range for the separation of DNA fragments up to 2000 bp [30]. The electrophoretic trace of DNA fragments after 20 min sonication was observed above traces of xylene cyanol, marker with which DNA of ~460 bp comigrates. Electrophoretic mobility of DNA sonicated 60 min was slightly lower than bromophenol blue marker, used for detection of DNA ~100 bp fragment length in this gel.

Most of the samples were prepared using the solution with DNA sonicated 20 min. The length of its fragments was determined from the average molecular weight M estimated by the intrinsic viscosity η of the DNA solution using the relation $\eta = 1.45 \times 10^{-6}\ M^{1.12}$ [31]. The value of the intrinsic viscosity was determined by a linear extrapolation to zero of the dependence on concentration of the partial viscosity. The partial viscosities were measured using a rotation viscosimeter AB-1 (Special Construction Bureau

of Biological Instrumentation, Russian Academy of Sciences, Pushchino, Russia) at concentrations between 0.1 and 1.5 mg/ml. By using this method, we determined the length of fragments ~600 bp in the solution of DNA sonicated 20 min.

Dioleoylphosphatidylcholine (DOPC, Avanti Polar Lipids, USA) at concentration 32 mg/ml was dispersed in a solution of 20 mM $CaCl_2$ or $MgCl_2$ dissolved in HEPES. The 0.5-mM HEPES buffer was used for the preparation of all solutions. The dispersion was vortexed and homogenized in an ultrasound bath and by at least threefold freezing–thawing process to obtain a homogeneous distribution of positive charge between lipid multilayers. A slightly opalescent dispersion of giant unilamellar vesicles was obtained (see Akashi et al. [16]).

Three following sets of samples were prepared: samples at molar ratio DNA/DOPC = 1:1 base/mol in 20 mM $CaCl_2$ (DNA/DOPC/Ca^{2+} = 1:1:4 base/mol/mol) with DNA fragments of diverse lengths; samples at molar ratio DNA/DOPC = 1:1 base/mol and concentration of cations in the range 0–76.5 mM, and samples with increasing concentration of lipid in the range DNA/DOPC ≤ 1:10 base/mol in 20 mM $CaCl_2$ solution. The last two sets of samples were prepared with DNA of ~600 bp fragments (20 min sonicated DNA).

The samples were prepared in the following way: the DNA solution and the DOPC dispersion were mixed at appropriate volume ratios to obtain the required molar ratio of DNA/DOPC. The concentration of lipid (4 mg/ml) was kept constant in each sample. The concentrated solution of cation^{2+} or 0.5 mM HEPES (or both) were added setting the required cation^{2+} concentration. The samples were vortexed for a short time; a few minutes after the preparation, a sediment is formed in the sample. The supernatant was gently removed by a Pasteur pipette and the sediment was placed between two Kapton foils (Dupont, France), which constitute the windows of the sample holder for X-ray diffraction. DOPC at concentration 32 mg/ml dispersed in the HEPES buffer was used for the preparation of samples of DOPC or DNA/DOPC = 1:1 base/mol without any cations. Each sample was let at rest at least 30 min before to be transferred to the sample holder.

2.2. X-ray diffraction

Small- (SAXD) and wide-angle (WAXD) synchrotron radiation diffraction experiments were performed at the soft-condensed matter beam line A2 at HASYLAB at the Deutsches Elektronen Synchrotron (DESY) in Hamburg (Germany), using a monochromatic radiation of wavelength $\lambda = 0.15$ nm. The evacuated double-focusing camera was equipped with two linear delay line readout detectors. The SAXD detector was calibrated using silver behenate [32] and the WAXD detector by tripalmitin [33,34]. The sample was equilibrated at each selected temperature for 5 min before exposure to radiation. Temperature scans were performed at a scan rate 1 °C/min and the diffractograms were recorded for 10 s every minute. Data reduction and normalization were done with the programs STAFO and OTOKO ([35,36] and references therein). Each diffraction peak of SAXD region was fitted with a Lorentzian $I = f(s)$ above a linear background. The Lorentzian is defined by

$$I = \frac{I_n}{1 + \left(\frac{S - S_n}{\Delta S_n}\right)^2} \quad (1)$$

where s_n ($n = 1, 2\ldots$) are the position of maxima, intensity I_n, the integral intensity Int_n and Δs_n the half-widths of the peak at half maximum. These parameters were determined using a non-linear least squares fitting program. All the measured WAXD patterns (not shown) exhibit one wide diffuse scattering peak characteristic of liquid-like carbon chains of phospholipid in the whole studied temperature range.

3. Results

3.1. DOPC multilamellar structure, effect of temperature

To study the structure of DNA + DOPC + cations^{2+}, it is necessary to know the structural parameters of the pure DOPC bilayer. DOPC in excess of aqueous phase forms a one-dimensional multilamellar L_α phase with the repeat distance d ~6 nm [37]. We observed two reflections in the SAXD pattern of DOPC at full hydration (Fig. 1a) with the repeat distance $d = 6.24 \pm 0.01$ nm at 20 °C. The repeat distance d is the sum

$$d = d_s + d_w \quad (2)$$

where d_s is the steric thickness of the lipid bilayer and d_w is the thickness of the water layer between bilayers; d_s includes molecules of water localized in the headgroup region of the lipid bilayer. The volume of water between two phospholipid molecules of adjacent bilayers is equal to the interbilayer separation (d_w) times the area per lipid molecule A_l. For zwitterionic lipids, the thickness d_w is the result of a balance between repulsive interbilayer interactions (steric, hydration and fluctuations) and attractive van der Waals forces [37]. From the thermodynamical point of view, lipids prepared in an excess of water are a two phase system, where the second phase is the bulk water. Not all the water that is added to the lipid is located between stacks of bilayers with uniform spacing and so there is a problem to determine the thickness d_s and the amount of water between opposite lipids bilayers as expressed in Eq. (2) [38,39].

The number of observed diffraction peaks of unoriented structures is reduced by the Lorentz factor, which decays as $1/s^2$. Fully hydrated lipid bilayers in the L_α phase show usually two, and at most three SAXD reflections, partly because of the large molecular and

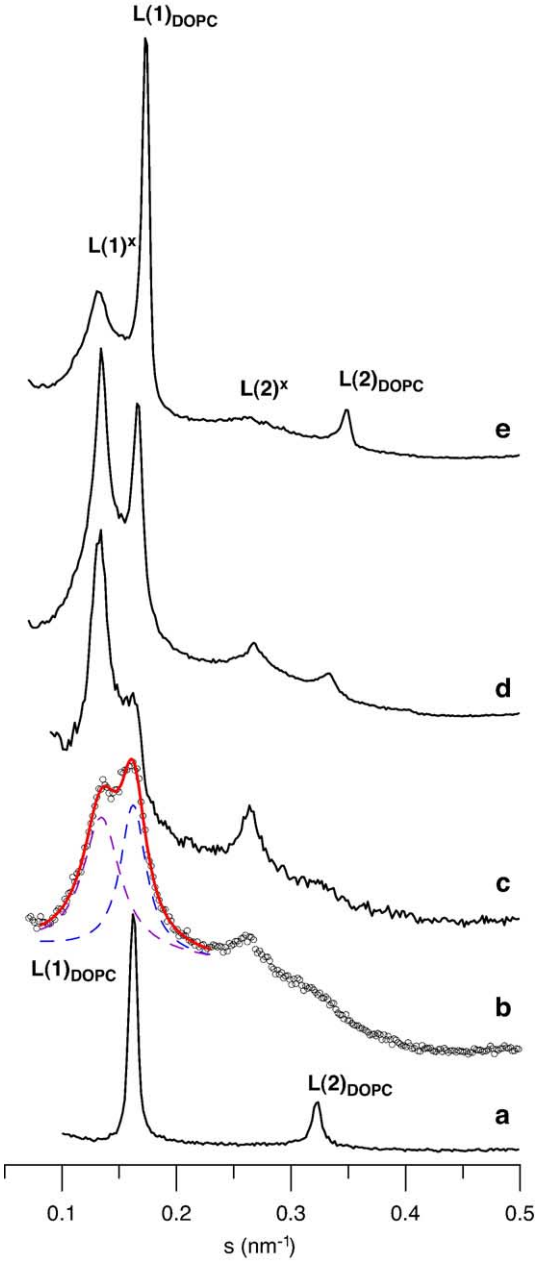

Fig. 1. SAXD patterns of DOPC multilamellar vesicles (a) and DOPC/DNA=1:1 mol/base aggregates at 20 °C prepared in: (b) 0 mM $MgCl_2$ or $CaCl_2$; (c) 2.5 mM $MgCl_2$; (d) 12.75 mM $CaCl_2$; (e) 51 mM $MgCl_2$ solution.

bilayer fluctuations which induce disorder and reduce the intensities of higher order reflections [37]. The electron density profiles calculated by using 2–3 orders of diffraction are not sufficiently accurate to determine the steric thickness of lipid bilayers. The problem of determination of the thickness of the lipid bilayer and of the area per lipid molecule of fully hydrated L_α bilayers was analysed in [37], where different methods are reviewed. In the present work we have used the values $d_s=4.69\pm0.01$ nm and $A_1=0.682\pm0.005$ nm^2 determined by SANS on unilamellar vesicles at 20 °C in our previous work [40]. These values are in good agreement with $d_s=4.67\pm0.22$ nm and $A_1=0.687\pm0.024$ nm^2 determined by SANS on DOPC unilamellar vesicles at 30 °C [41], and also with $d_s=4.53$ nm and $A_1=0.722$ nm^2 at 30 °C reported in the SAXD work [37,39]. The thickness of the aqueous layer calculated as $d_w=d-d_s\sim 1.24$ nm is the so-called steric water thickness [37] that separates lipid bilayers. The d_w value depends not only on temperature but may depend as well on the method of preparation and history of the sample because multilamellar vesicles in a random dispersion are certainly polydisperse. The swelling of such structures due to temperature changes might be non-uniform.

In the range 20–80 °C, the repeat distance of the DOPC bilayer stacking increases with temperature (Fig. 2A). The transversal thermal expansion coefficient at constant pressure π determined from

$$\alpha=\frac{1}{d}\left(\frac{\partial d}{\partial T}\right)_\pi \tag{3}$$

where T is the absolute temperature, is obtained by a linear least square fitting of the data in the range 20–60 °C (Table 1). In the fluid lamellar L_α phase, a temperature increase induces an increase of the population of *gauche* conformers in lipid acyl chains accompanied by the lateral expansion of the bilayer, what is manifested by a decrease of the lipid thickness [42,43]. It enhances also fluctuations of the lipid bilayer which are accompanied by a diffusion of water molecules from the bulk water phase in between lipid

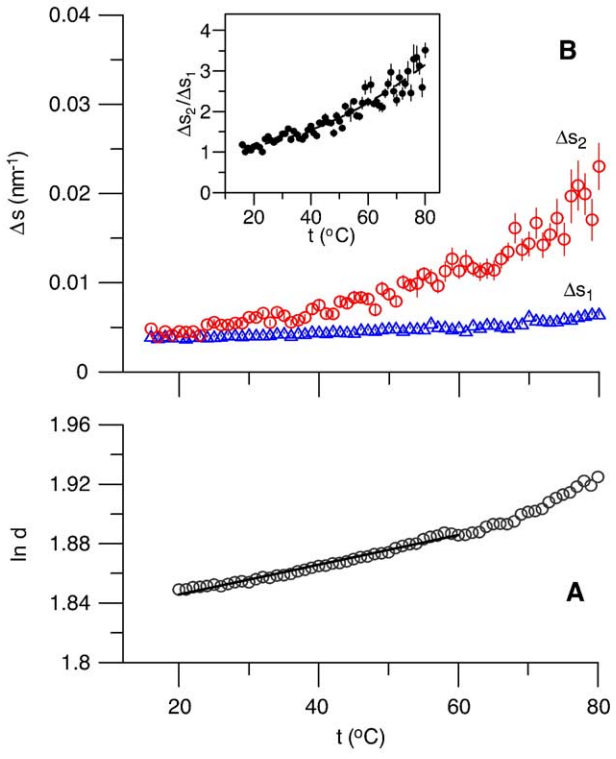

Fig. 2. (A) Temperature dependence of the repeat distance d (in nm) of multilamellar DOPC vesicles; (B) the first order Δs_1 and the second order Δs_2 Bragg reflection widths of DOPC; inset: the ratio $\Delta s_2/\Delta s_1$.

Table 1
Repeat distances at 20 °C (d_{20}) and transversal thermal expansion coefficients (α) of the L^x and L_{DOPC} phases of DNA+DOPC+Ca^{2+} aggregates

DNA:DOPC base/mol	Ca^{2+} mM	t (°C)	L^x phase		L_{DOPC} phase	
			d_{20} (nm)	$10^5\alpha$ (K^{-1})	d_{20} (nm)	$10^5\alpha$ (K^{-1})
0:1	0	20–60			6.24±0.01	100±2
1:1	0	20–80	7.78±0.01	−75±3	6.45±0.06	−43±4
1:1	12.75	20–80	7.44±0.01	−83±1	6.05±0.01	–
1:1[a]	12.75	20	7.57±0.01	–	6.29±0.01	–
1:1	51	20–55	7.39±0.09	−46±4	5.75±0.01	−54±5
1:1	51	56–80		−85±4		−54±5
1:1[b]	20	20–80	7.46±0.01	−83±1	6.00±0.01	−31±2

[a] Data determined after heating scan.
[b] DNA highly polymerized.

bilayers, thus an increase of d_w [44]. The one of these two processes that prevails determines the direction of the change in the lipid repeat distance.

Fully hydrated lipid bilayers are characterized by a wide array of fluctuations resulting in changes in the intensity, width and number of observable diffraction reflections as reviewed in [37]. Molecular disorder and fluctuations give rise to the so-called short-range fluctuations which are intrinsic to single lipid bilayer. They correspond to disorder within a unit cell in a stack of repeat units. Long-range fluctuations are fluctuations in the relative positions of the unit cells. This disorder is a consequence of undulations of bilayers, induced by temperature and enhanced by changes of the bilayer bending modulus. Both kinds of fluctuations change the shape of the peaks from the ideal delta function by removing intensity from the central scattering peak and spreading it into tails of diffuse scattering centred at the peak positions. The importance of such smearing intensity is larger at high diffraction orders [37,44,45]. In the present paper, we have observed a broadening of the first and second order diffraction peaks of DOPC when temperature increases (Fig. 2B). The width of the second order Bragg peak Δs_2 and the ratio of the widths of second and first Bragg diffraction peaks $\Delta s_2/\Delta s_1$ increase nonlinearly with temperature (Fig. 2B, inset). This is an evidence that the disorder induced by undulations increases at higher temperature.

3.2. DOPC multilamellar structure in presence of DNA

The diffraction pattern of DOPC multilamellar mixture changes when DNA is added, even in absence of metal cations (Fig. 1b). The diffractograms were identified as a superposition of two one-dimensional periodic structures. The reflections $L(1)_{DOPC}$ and $L(2)_{DOPC}$ with the position of the first order maximum $s=0.162$ nm^{-1}, close to the position of the first order maximum of multilamellar DOPC structure ($s=0.160$ nm^{-1}), were identified as reflections due to the DOPC bilayer stacking (L_{DOPC}). The reflections $L(1)^x$ and $L(2)^x$ were identified as two reflections of another lamellar phase (L^x). There are two possible interpretations of phase L^x: (a) another lamellar DOPC phase resulting from the non-homogeneity of the sample, or (b) DOPC bilayers with DNA polyanions intercalated in water layers between the bilayers.

The positions of the maxima were determined by fitting the experimental points by a superposition of two Lorentzians above a linear background as depicted in Fig. 1b. The repeat distances of both phases, determined from $d=1/(s_2-s_1)$, are $d_{Lx}=7.78\pm0.01$ nm and $d_{DOPC}=6.45\pm0.06$ nm at 20 °C. We did not find any information in the literature about the effects of DNA polyanion on the lipid bilayer thickness without presence of other additives. Consequently, we suppose that the DOPC bilayer thickness does not change. By subtracting the thickness of lipid bilayer $d_s=4.69\pm0.01$ nm, we obtained the interbilayer distances of the two phases: $d_{wLx}=3.09\pm0.02$ nm and $d_{wDOPC}=1.76\pm0.07$ nm. The repeat distance d_{Lx} and the corresponding interbilayer distance are too large for bilayers formed by a zwitterionic lipid like DOPC. Interbilayer distances of these dimensions (~2–3 nm) were observed only with charged bilayers [46]. However, considering the transverse dimension of hydrated DNA (diameter 2.4 nm [6]), we see that it can easily fit between the lipid bilayers. Its presence could even further increase d_w because of the electrostatic repulsion between phosphate fragments of the lipid and DNA.

The positions of reflections and their intensities change with increasing temperature, but both lamellar phases are present in the whole studied temperature range 20–80 °C. The transversal thermal expansivities of both phases, determined in the range 20–80 °C according to Eq. (3), are reported in Table 1. Large differences in transversal thermal expansivities of both phases ($\alpha_{Lx}=-(75\pm3)$ 10^{-5} K^{-1} and $\alpha_{DOPC}=-(43\pm4)$ 10^{-5} K^{-1}) confirm that the diffractogram in Fig. 1b represents two lamellar phases of different compositions. Francescangeli et al. [25] did not observe any changes in the DOPC diffractogram when DNA was added to the DOPC multilamellar vesicles. However, the interaction of DNA with lipid bilayers, even in absence of cationic surfactants or metal cations was observed in calorimetric experiments [11,18,19,47]. In our previous work [48], we did not observe any change in diffractograms of dilauroylphosphatidylcholine (DLPC) in presence of DNA, but there were changes in the trans-

versal thermal expansion of DLPC bilayer in presence of DNA.

3.3. DOPC multilamellar structure in presence of DNA and divalent cations

We observed significant changes in the diffraction pattern of DNA+DOPC mixture already at very low concentrations of divalent ions Mg^{2+} or Ca^{2+} as illustrated by diffractograms of DNA/DOPC=1:1 base/mol aggregates prepared in 2.5 mM Mg^{2+} (Fig. 1c) and also in 12.75 mM Ca^{2+} (Fig. 1d). The aggregates formed in presence of Ca^{2+} ions show diffractograms similar to those of aggregates created in presence of Mg^{2+}: 2–4 reflections of L^x phase and 2 reflections of L_{DOPC} phase. Occasionally, we identified a third-order reflection of L_{DOPC} phase. The number of reflections, their intensities and widths for both phases depend on the concentration of divalent ions in the sample, as documented below. In contrast, within the studied temperature range, we did not observe any reflection due to DNA. The SAXD diffractograms are similar for samples prepared about 30 min before exposition to X-ray or 10 days old, the only difference being a slightly higher Δs in freshly prepared samples.

The repeat distances of L^x and L_{DOPC} phases determined from $d=1/(s_2-s_1)$, as a function of the cation concentration are shown in Fig 3. The dependence of the repeat distance d_{Lx} with ion concentration is slightly different for Ca^{2+} and Mg^{2+} ions. Increasing amounts of Ca^{2+}, induce a decrease of d_{Lx}, steep at low concentrations (by 0.34 nm at 12.75 mM Ca^{2+}) and smoother subsequently. The uncertainty of d_{Lx} due to the analysis of the data is 0.03 nm.

The behaviour of d_{Lx} is the same for samples containing Mg^{2+} up to 40.8 mM, then it increases as well as the uncertainty about the position of the second reflection, due to low resolution, as one can see on the diffractogram of DNA/DOPC=1:1 base/mol aggregate prepared in a 51 mM solution of Mg^{2+} (Fig. 1e).

The behaviour of phase L^x with ion concentration depicted in Fig. 3 differs from the behaviour of pure phospholipids in presence of divalent cations. Significant changes in the SAX diffraction pattern of neutral phospholipid bilayers with Ca^{2+} and Mg^{2+} have been documented in [14] and [15]: the addition of 1 mM $CaCl_2$ destroys the lamellar structure of neutral phosphatidylcholines and makes it to swell into excess water. The lamellar phase reappears when the concentration of $CaCl_2$ further increases. A partially disordered lamellar phase with the repeat distance 15–20 nm appears at about 10 mM, and d ~9–10 nm at 100 mM. Akashi et al. [16] have shown that 1–30 mM solution of Ca^{2+} or Mg^{2+} promotes the formation of giant unilamellar vesicles. At concentration above 50 mM, the population of vesicles decreases.

Our experimental data can be explained by the following model of the L^x phase: DNA intercalates in water layers between lipid bilayers (so-called sandwich structure) and the binding between lipid bilayers and DNA polyanion is mediated by divalent cations. As reported in [49,50], the binding site for cations is near the negative phosphate group of the P^-–N^+ dipole of phospholipid headgroup. The observed decrease of d_{Lx} spacing compared to DOPC+DNA samples without cations is then a result of the electrostatic screening of repulsion between phosphate fragments of DOPC and DNA by metal ions. Tatulian et al. ([15] and references therein) did not observe any changes of bilayer thickness of DPPC upon changing the concentration of $CaCl_2$ within an accuracy ±0.2 nm. Assuming the same for DOPC, we get the interbilayer distance $d_{wLx}=d_{Lx}-d_s$ ~2.9 nm. This value of d_{wLx} offers enough space for the intercalation of DNA strands with diameter 2.4 nm and hydrated divalent metal ions. Furthermore, the repeat distance d_{Lx} ~7.4–7.5 nm observed in the middle of Ca^{2+} concentration range is in accord with the value of $d=7.67\pm0.05$ nm determined for lipid bilayer spacing in DNA+DPPC+Mg^{2+} aggregates in the liquid crystalline phase of DPPC reported in our previous work [13]. McManus et al. [24] studied DNA+DPPC+Ca^{2+} aggregates at Ca^{2+} concentrations of 1–100 mM and found the repeat distance in the range ~7.35–7.65 nm in the fluid phase.

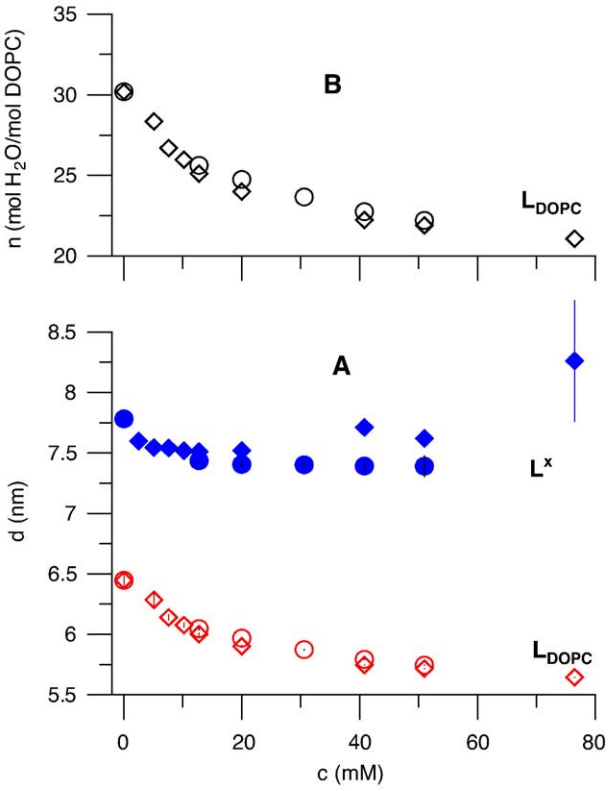

Fig. 3. (A) Dependences of the L^x and L_{DOPC} repeat distances on the cation^{2+} concentration in DOPC+DNA+Ca^{2+} (●,○) and DOPC+DNA+Mg^{2+} (♦,◇) aggregates at DOPC/DNA=1:1 mol/base and 20 °C. (B) Dependence of the number of water molecules per DOPC molecule on the cation^{2+} concentration of L_{DOPC} phase in DOPC+DNA+cation^{2+} aggregates (○—Ca^{2+}; ◇—Mg^{2+}).

The repeat distance of L_{DOPC} phase decreases non-linearly in the same way for both Ca^{2+} and Mg^{2+} in the whole studied concentration range, starting at 6.45±0.06 nm at zero cation concentration and reaching 5.65±0.01 nm at 76.5 mM of Mg^{2+} (shown in Fig. 3). Supposing no changes of the DOPC bilayer thickness, the observed repeat distance decrease probably results from the decrease of the thickness of the water layer ($\Delta d_{wDOPC} \cong \Delta d_{DOPC}$). The changes in the hydration of the bilayer can be expressed by the number of water molecules per DOPC molecule. As mentioned above, water molecules are localized inside the polar part of the bilayer (n_w) and also in the space between opposite bilayers (n'_w). Tristram-Nagle et al. [39] determined the volume of the DOPC molecule at 30 °C, $V_{30\ °C}$= 1.3033 nm^3, and the thermal volume expansion coefficient β=0.0008 K^{-1}. Applying these data, we calculated the volume of the DOPC molecule at 20 °C, $V_{20\ °C}$=1.2929 nm^3. From d_s and A_l, the number of water molecules per DOPC localized inside the polar parts of the bilayer is $n_w=((d_s A_l/2)-V_{20\ °C})/V_w$, where V_w=0.02997 nm^3 is the molecular volume of water at 20 °C. We obtained n_w=10.2±0.5 molecules of water per DOPC, in accord with n_w=11 determined in [39] at 30 °C. The steric thickness of water layers is $d_w=d_{DOPC}-d_s$=1.76±0.07 nm at zero cation concentration. Then, the number of water molecules per DOPC (n'_w) localized between adjacent lipid bilayers is $n'_w=A_l d_w/(2.V_w)$=20±1. We found that at zero concentration of cations the total number of water molecules per DOPC molecule at 20 °C is $n_w+n'_w$=30.2±1.5. This value is close to $n_w+n'_w$=32.5 determined at 30 °C in [39]. The decrease in hydration of DOPC with increasing concentration of cations is depicted in Fig. 3B. The largest change of the repeat distance, Δd_{DOPC}= 0.80±0.07 nm at 76.5 mM Mg^{2+}, corresponds to a removal of ~9±1 water molecules per DOPC from the interbilayer space. Two steps of the hydration process of phosphatidylcholine bilayers in the liquid crystalline phase are known: approximately 10–12 molecules of water per molecule of lipid tightly bind to the lipid head group (n_w) and this hydration is accompanied by a dramatic decrease of the thickness of the lipid bilayer and an increase of the area per molecule (so-called inner water). Further water molecules (n'_w ~12–22) are located in the fluid space between adjacent bilayers [39,51,52]. This "outer waters" are much more weakly bound and it requires a small fraction of thermal energy (about 0.1 kJ/mol) to remove an outer water molecule in comparison with over 4 kJ/mol needed to remove inner water [53]. Our analysis indicates a dehydration of the outer water layer of DOPC in DNA+DOPC+$cation^{2+}$ aggregates.

The existence of a phosphatidylcholine phase with limited hydration in samples prepared in excess of water is rather surprising. We have devoted more attention to the analysis of the diffractograms to obtain more information about DNA+DOPC+$cation^{2+}$ aggregates characterized by the coexistence of two phases.

When the interbilayer spacing exceeds 1 to 2 nm, the thermally induced undulations or fluctuations of the lipid bilayer are not negligible because of changes in the bilayer bending modulus or in the curvature elastic modulus [44]. These long-range fluctuations and also short-range fluctuations affect the widths of Bragg diffraction peaks (see Fig. 2B). We investigated how much the widths of Bragg diffraction peaks depend on the presence of metal cations.

The dependence of the widths of the first reflections Δs_{1Lx} and Δs_{1DOPC} on the concentration of Ca^{2+} ions is shown in Fig. 4A. The width of Δs_{1Lx} depends on the ion concentration quasi-parabolically with a minimum at ~20 mM Ca^{2+} (Fig. 4A, empty circles). The width Δs_{2Lx} of the second peak of L^x phase shows qualitatively a similar dependence (not shown). At zero concentration of metal cations, the electrostatic repulsion between the phosphate fragments of DOPC polar groups and DNA polyanion induces a fluctuation of bilayers which explains the width of the diffraction peaks. The width Δs_{1Lx} decreases with increasing concentration of Ca^{2+} ions up to ~20 mM. Divalent cations stabilize the bilayer fluctuations by electrostatic screening of the repulsion between DNA and lipid, yielding the narrowing of the peaks. Further increase of Ca^{2+} concentration in the interlamellar space induces a positive surface charge on adjacent bilayers and enhances

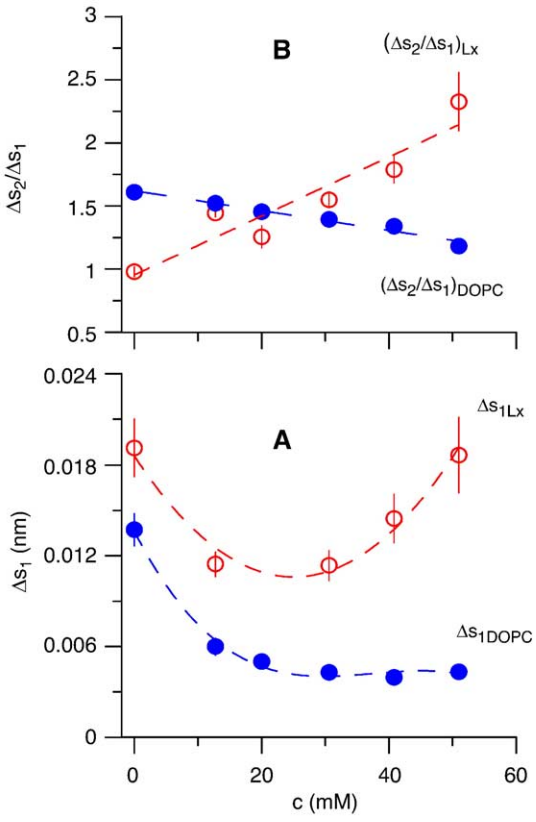

Fig. 4. (A) Dependence of the first order Bragg reflections widths of L^x (○) and L_{DOPC} (●) phase; (B) the ratio of the widths of second and first reflections $\Delta s_2/\Delta s_1$ of L^x (○) and L_{DOPC} (●) phase on the Ca^{2+} concentration in DOPC/DNA=1:1 mol/base aggregates at 20 °C.

fluctuations, manifested by the increase of Δs_{1Lx} at $\geq$30.6 mM Ca^{2+}. An evidence of this positional disorder induced by the increase of ion concentration is also documented in Fig. 4B. The ratio of the widths of the second and first diffraction peaks $\Delta s_{2Lx}/\Delta s_{1Lx}$ strongly increases. On the other hand, the width of the first reflection of L_{DOPC} phase, Δs_{1DOPC}, decreases nonlinearly in the whole studied concentration range (Fig. 4A, full circles). The ratio $\Delta s_{2DOPC}/\Delta s_{1DOPC}$ also decreases with increasing concentration of Ca^{2+} ions (Fig. 4B) what reflects a reduction in fluctuations of DOPC bilayers as a result of dehydration of interlamellar space (Fig. 3). The intensities of the first reflections and the total integral intensities (sum of integral intensities of the first and second reflection) for both phases L^x and L_{DOPC} display also a quasi-parabolic dependence on the concentration of Ca^{2+} ions with a maximum at ~20 mM Ca^{2+} (not shown). Our experimental results thus indicate that 20 mM Ca^{2+} is the optimal concentration of cations for screening electrostatic repulsion between DNA polyanion and DOPC bilayers in DNA/DOPC=1:1 base/mol aggregates. Aggregates prepared at lower concentrations of Ca^{2+} show an increase of lipid bilayers fluctuations because of insufficient screening of negative charges. Too high concentrations of Ca^{2+} ($\geq$30.6 mM) induce additional fluctuations because of an excess of positive charge between lipid bilayers.

We have observed similar dependences for aggregates created in presence of Mg^{2+} ions, except that the minimum of the width Δs_{1Lx} was shifted to ~10 mM Mg^{2+}.

3.4. Temperature behaviour of DNA+DOPC+Ca^{2+} aggregates

We studied the thermal stability of aggregates in the temperature range 20–80 °C at two concentrations: 12.75 and 51 mM Ca^{2+}. The SAXD patterns were measured during the heating scans.

Diffractograms of the DNA/DOPC=1:1 base/mol aggregate in 12.75 mM Ca^{2+} at 20, 75 and 90 °C are shown in Fig. 5a–c. The diffraction pattern change with temperature: the intensity of the first order reflection of the L_{DOPC} phase decreases (Fig. 5b), the second order diffraction peak of L_{DOPC} phase becomes broader at 75 °C, but the aggregate still keeps its organization. After the scan, the sample was heated to 90 °C and equilibrated for 20 min. The diffractogram is shown in Fig. 5c. Broad diffraction peaks are superimposed to a diffuse scattering and the second order diffraction peaks are totally absent. After this heating procedure, the sample was slowly cooled and was again exposed 8 h later (Fig. 5d). As it follows from Fig. 5d, the aggregate exhibits high temperature stability, though some hysteresis is observed. The widths of first order reflections of both phases increase by ~50%. Repeat distances are given in Table 1.

The bilayer spacing d_{Lx} decreases in the studied temperature range (Fig. 6A). From these data, we determined the

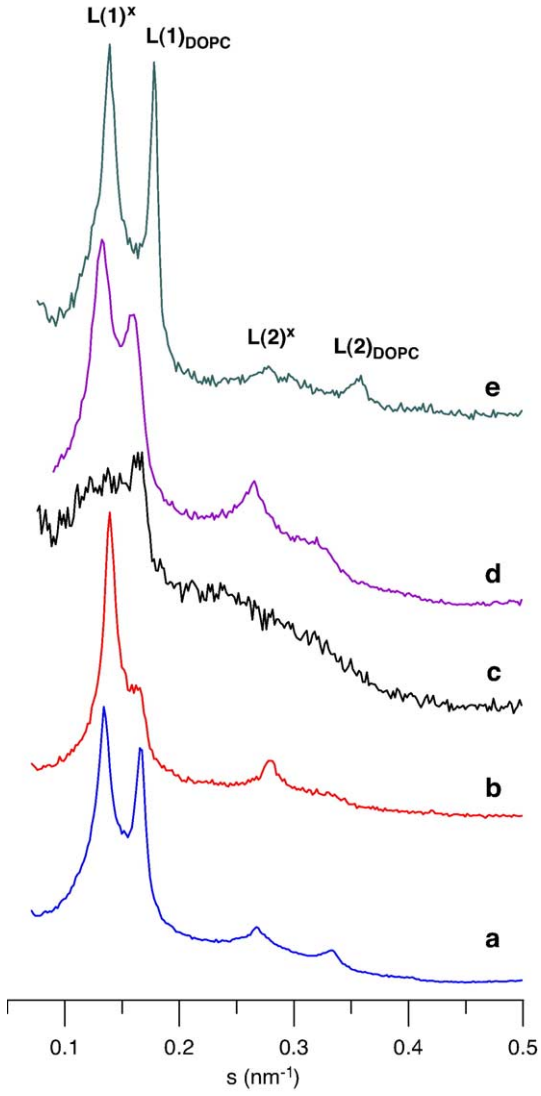

Fig. 5. SAXD patterns of DOPC/DNA=1:1 mol/base aggregates in 12.75 mM Ca^{2+} at (a) 20 °C; (b) 75 °C; (c) 90 °C; (d) 20 °C and (e) DOPC/DNA=1:1mol/base aggregate in 51 mM Ca^{2+} at 75 °C.

transversal thermal expansion coefficient $\alpha_{Lx}=-(83\pm1)\ 10^{-5}\ K^{-1}$ (Table 1). The change of the repeat distance, $\Delta d_{Lx}=d_{L20}-d_{L80}=0.37\pm0.02$ nm, where d_{L20} and d_{L80} are the repeat distances of L^x phase at 20 and 80 °C, respectively, is similar to the value observed for DNA+DOPC, $\Delta d_{Lx}=d_{L20}-d_{L80}=0.33\pm0.02$ nm. We observed a slight decrease of the width of the first order reflection Δs_{1Lx} when temperature increases; the ratio of the widths of the second and first reflections $\Delta s_{2Lx}/\Delta s_{1Lx}$ increases only slightly with temperature (Fig. 6C, empty circles). Comparing the ratio $\Delta s_{2Lx}/\Delta s_{1Lx}$ of L^x phase of DNA+DOPC+Ca^{2+} aggregates with that obtained for pure DOPC bilayer stacking (Fig. 2), it is evident that the thermally induced long-range fluctuations observed in pure DOPC are damped by the DNA intercalated between bilayers. The observed decrease of the repeat distance $\Delta d_{Lx}=0.37$ nm indicates that the temperature-induced decrease of the

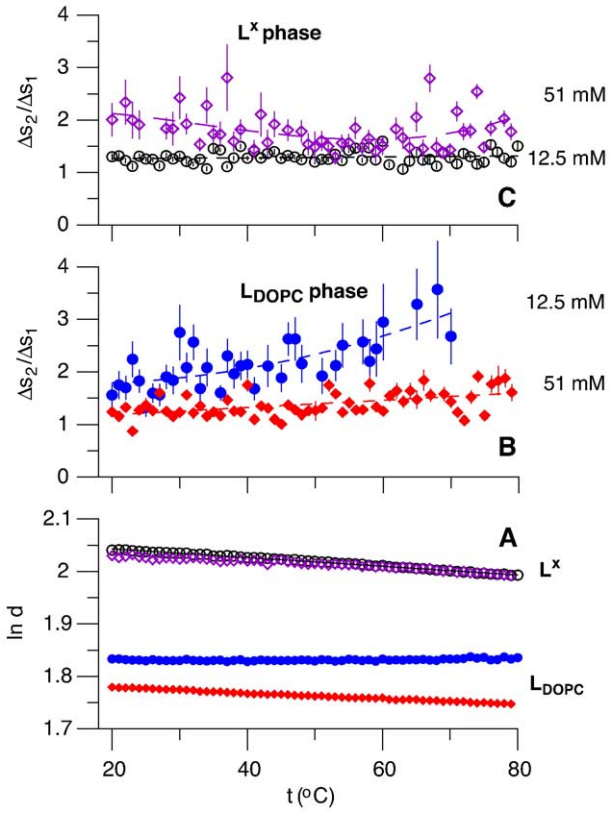

Fig. 6. (A) Temperature dependence of the repeat distance (in nm) of L^x (○, ◇) and L_{DOPC} (●, ◆) phases DNA/DOPC=1:1 base/mol aggregate in 12.75 mM Ca^{2+} (○, ●) and 51 mM Ca^{2+} (◇, ◆); (B) the ratio of the widths of second and first reflections $\Delta s_2/\Delta s_1$ of L_{DOPC} phase of aggregates in 12.75 mM (●) and 51 mM (◆) Ca^{2+}; (C) the ratio $\Delta s_2/\Delta s_1$ of L^x phase of aggregates in 12.75 mM (○) and 51 mM (◇) Ca^{2+}.

thickness of the lipid bilayer prevails against the diffusion of water molecules from the bulk water phase in between lipid bilayers. The same effect, i.e., the decrease of the repeat distance and of the temperature-induced long-range fluctuations in comparison with pure lipid multibilayers, was also observed in the ternary system DNA+DLPC+cationic gemini surfactant [48].

We have observed only minor changes of the repeat distance of L_{DOPC} phase in the temperature range 20–80 °C, as shown in Fig. 6A (full circles). The mean value of the repeat distance is $d_{DOPC}=6.25$ nm with a standard deviation ± 0.01 nm, but a more accurate observation detects values out of this range at the edges of the studied temperature range. Such fluctuations prevent the evaluation of the transversal thermal expansion coefficient with a satisfactory precision. Also, the ratio of the widths of the second and the first order reflection $\Delta s_{2DOPC}/\Delta s_{1DOPC}$ (Fig. 6B, full circles) increases with increasing temperature what characterizes the increase of the long-range disorder of bilayers. This effect is more pronounced at high temperature. Above 70 °C, the second reflection was too broad and practically merged into the diffuse scattering. Fluctuations of bilayers induced by temperature probably allow water molecules to penetrate between lipid bilayers. The consequent increase of the thickness of water layers compensates the concomitant decrease of the thickness of lipid bilayers.

With increasing concentration of ions, the level of organization and the temperature stability of L_{DOPC} phase improve. A typical diffractogram of DNA+DOPC+Ca^{2+} aggregates in 51 mM Ca^{2+} at 75 °C is shown in Fig. 5e. The transversal thermal expansion coefficient $\alpha_{DOPC}=-(54\pm0.5)\ 10^{-5}\ K^{-1}$ was calculated from a temperature scan (Table 1). This value is smaller than that of pure DOPC bilayers and of aggregates prepared at lower concentrations of Ca^{2+} ions (see Table 1), indicating a higher resistance of lipid bilayers against water diffusion from the bulk aqueous phase. When we compare the temperature dependence of the ratio $\Delta s_{2DOPC}/\Delta s_{1DOPC}$ in Fig. 6B (full squares) with that observed for aggregates prepared at low concentrations of Ca^{2+} or without Ca^{2+} (Fig. 6B, full circles and Fig. 2B), the higher level of organization of lipid bilayers is evident. As it was mentioned above, the increase of temperature induces bilayer undulations and changes of the bilayer bending modulus (long-range disorder). The excellent temperature stability of L_{DOPC} phase and the damped temperature-induced long-range fluctuations indicate that this phase is partially dehydrated (see Fig. 3B).

The temperature behaviour of the L^x phase in aggregates prepared in 51 mM Ca^{2+} is different. Two regions with different transversal thermal expansions can be distinguished in Fig. 6A (empty squares). While in the temperature range 20–55 °C we have found the transversal thermal expansion coefficient $\alpha_{1Lx}=-(46\pm4)\ 10^{-5}\ K^{-1}$, at $t>55$ °C, within the experimental error, both d_{Lx} spacing and transversal thermal expansion coefficient ($\alpha_{2Lx}=-(85\pm4)\ 10^{-5}\ K^{-1}$) are the same as in aggregates prepared at low ion concentration. With increasing temperature, the ratio $\Delta s_{2Lx}/\Delta s_{1Lx}$ is very scattered (Fig. 6C—empty squares), what is in contrast with the highly organized L_{DOPC} phase in the same aggregates. The concentration of Ca^{2+} cations in the interlamellar space of the L^x phase is higher than that necessary for the electrostatic screening of the repulsion between the DNA polyanion and DOPC phosphate fragments. The excess of Ca^{2+} creates a positive charge at the bilayer surface and gives rise to fluctuations of bilayers (as indicated also in Fig. 4) which are then enhanced by the temperature increase.

3.5. DNA+DOPC+Ca^{2+} aggregates, effect of DNA length

In order to obtain more detailed information about the coexistence of phases L^x and L_{DOPC}, we prepared aggregates DNA/DOPC=1:1 base/mol in 20 mM $CaCl_2$ with DNA fragments of different lengths. Highly polymerized DNA was sonicated 0–3600 s as described in Materials and methods. Using the sonication procedure, the mean length of fragments was changed from approximately 12 kbp (highly polymerized DNA) to ~100 bp. All samples were incubated 10 days at 5 °C before exposure. We observed changes of the number of diffraction reflections, of their

widths and intensities, but no changes of the positions of reflections and number of phases. Aggregates formed with highly polymerized DNA or by its long fragments (200–400 s of sonication) have shown high quality diffractograms with four reflections of L^x phase and 2–3 reflections of L_{DOPC} phase, what indicates a well-organized structure. A typical diffractogram of an aggregate created with DNA sonicated longer than 600 s shows the first and the second order reflections of both L^x and L_{DOPC} phase (see Fig. 1c–e). The repeat distance $d_{Lx}=7.45\pm0.02$ nm of L^x phase is the result of an average of seven diffractograms of aggregates prepared with DNA fragments of different length. The repeat distance of the L_{DOPC} phase determined in the same way is $d_{DOPC}=5.93\pm0.05$ nm. Changes of the intensities of diffraction peaks enable the calculation of the fraction of L^x phase (X_{Lx}) as a function of the length of DNA fragments (characterized by the sonication time). X_{Lx} is calculated as the ratio between the total integral intensity of L^x phase and the sum of the total integral intensities due to both phases:

$$X_{Lx}=\frac{\sum_{n=1}^{2}\mathrm{Int}_{Lx,n}}{\sum_{n=1}^{2}\left(\mathrm{Int}_{Lx,n}+\mathrm{Int}_{DOPC,n}\right)} \quad (4)$$

where Int is the integral intensity of the n^{th} ($n=1$, 2) order reflection, and indices Lx and DOPC indicate the L^x and L_{DOPC} phases, respectively. With increasing time of sonication (decreasing length of DNA fragments), we observed a decrease of the fraction of L^x phase as shown in Fig. 7A. At the molar ratio DNA/DOPC=1:1 base/mol, practically all lipid is incorporated in the DNA+DOPC+Ca^{2+} aggregates (see experimental results below). It is known that cationic vesicles or surfactants bind to the DNA polyanion in a cooperative manner [54]. The decrease of the fraction of the L^x phase indicates that the binding affinity of DNA for DOPC in presence of Ca^{2+} probably increases with the length of the fragments. Conversely, the fraction of the L_{DOPC} phase, $X_{DOPC}=1-X_{Lx}$, is larger when the DNA fragments are shorter, in the range X_{DOPC} ~0.15–0.55 (not shown). We found that these changes of the amount of each phase are accompanied by changes in the degree of long-range disorder of the L_{DOPC} phase, monitored by the ratio $\Delta s_{2DOPC}/\Delta s_{1DOPC}$ ratio (Fig. 7B). With a larger fraction of L_{DOPC} phase in the aggregate, the disorder in the relative positions of its unit cells decreases, indicating restrictions to undulatory fluctuations.

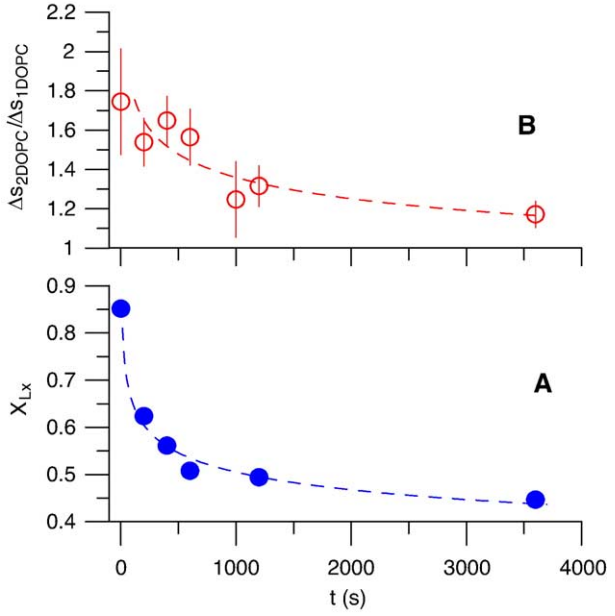

Fig. 7. (A) Dependence of the fraction X_{Lx} of L^x phase of DOPC/DNA=1:1 mol/base aggregates in 20 mM Ca^{2+} on the DNA fragments length expressed as the time of sonication of highly polymerized DNA. (B) Ratio of the widths of second and first order reflections $\Delta s_2/\Delta s_1$ of L_{DOPC} phase.

3.6. DNA+DOPC+Ca^{2+} aggregates, effect of increasing lipid concentration

We determined the concentration of DNA in the excess water phase of the DNA/DOPC=1:1 base/mol aggregate in 20 mM $CaCl_2$ in order to find out how much DNA is trapped in the aggregate between the lipid lamellae. The DNA concentration was determined spectrophotometrically from the absorbance at 260 nm. We found that at least ~20% of DNA was located in the sedimented aggregate. Increasing the DOPC/DNA molar ratio, the portion of bound DNA increases, as shown in Fig. 8.

It is known that supramolecular aggregates like vesicles, micelles, etc. affect the background of UV-VIS spectra because of the light scattered by them. This effect increases with λ^{-4} and with the size of the aggregates. We did not observe any changes in the background of the absorbance dependence $A=f(\lambda)$ as long as DOPC/DNA < 6:1 mol/base. At higher molar ratios, the contribution from light scattering was eliminated numerically according to [55] with the aim to determine the correct value of DNA absorbance. The high portion of unbound DNA in the supernatant and the absence of "unbound lipid" in the sample prepared at 20 mM Ca^{2+} motivated us to investigate structural changes of aggregates with increasing DOPC/DNA molar ratio.

Samples were prepared in the range of molar ratios DOPC/DNA ≤ 10:1 mol/base in 20 mM Ca^{2+}. The diffractograms show practically no changes in the position of reflections (Fig. 9a–e) in the whole studied range of DOPC/DNA molar ratios. The average values of repeat distances of both phases are $d_{Lx}=7.53\pm0.07$ nm and $d_{DOPC}=5.94\pm0.03$ nm. The increase of lipid content in the samples only slightly affected the width of the first reflection of L_{DOPC} phase, but we observed changes of the intensity and a marked broadening of the first order reflection of the L^x phase, as shown in Fig. 9a–e.

Total integral intensities of L^x and L_{DOPC} phase were used for the evaluation of the changes observed in diffractograms. With increasing DOPC/DNA molar ratio,

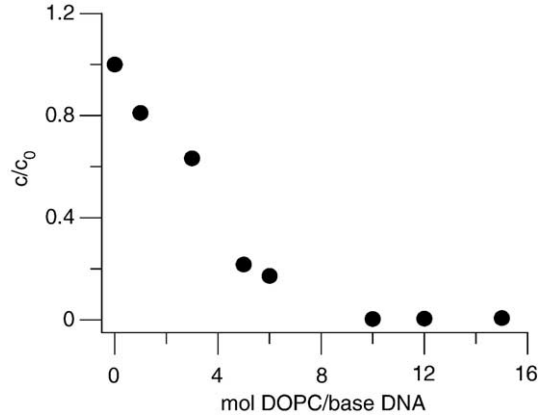

Fig. 8. Dependence of the ratio c/c_0 on the DOPC/DNA molar ratio (at 20 mM $CaCl_2$), c_0 is the DNA concentration before aggregate formation and c is the DNA concentration in the sample supernatant after the aggregate formation.

the total integral intensities of both the L^x and L_{DOPC} phases show a quasi-parabolical pattern with a maximum at ~5 molecules DOPC per DNA base (Fig. 9, inset). The ratio DOPC/DNA=5:1 mol/base is in good agreement with the observed 20% decrease in the DNA concentration in the supernatant after formation of DOPC/DNA=1:1 mol/base aggregate and probably indicates the optimal binding ratio of DNA to DOPC molecules in presence of Ca^{2+} ions. Kharakoz et al. [56] found the stoichiometry of binding about 4.5–5 lipid molecules per nucleotide in DNA-DPPC aggregates prepared in 22 mM $CaCl_2$ in a temperature-scanning ultrasonic study. Fig. 9 (inset) shows that the total integral intensity of L_{DOPC} phase displays the same quasi-parabolic trend as in the L^x phase, indicating that the ratio between the fractions of each phase, X_{DOPC}/X_{Lx} ~0.5, is constant. Our samples were prepared at constant Ca^{2+} concentration 20 mM and the amount of DOPC (hydrated with the solution of ions) in each sample was kept constant. The amount of DNA in the sample decreases with increasing DOPC/DNA molar ratio. The excess of lipid in the samples, which is not incorporated in the aggregate, forms unilamellar vesicles in presence of Ca^{2+} ions which are located in the supernatant and, consequently, do not affect the diffraction pattern of the aggregate.

4. Discussion

DNA aggregates with cationic vesicles create a condensed fluid lamellar phase L_α^c where parallel DNA strands are intercalated between lipid bilayers and packed in a one-dimensional periodical lattice [6,48,57–59]. This organization of DNA strands results in one broad reflection in SAX region which usually has lower intensity in comparison with the intensity of reflections due to lipid bilayer stacking. In contrast, we did not observe any DNA reflection in our diffractograms. In our previous work [13], we observed one broad reflection identified as a diffraction peak from DNA packing in a one-dimensional periodical lattice between lipid bilayers in the DNA/DPPC/Mg^{2+}=1:1:5 base/mol/mol aggregate. The SAX diffraction pattern shows the sandwich structure of the aggregate, and only one lipid phase was observed. The lattice parameters d_{DNA}=6.35±0.16 nm and d_{DNA}=6.12±0.07 nm in the gel and the liquid–crystalline phase were determined at 28 and 53 °C, respectively. These experiments indicate the ability of divalent cations to pack DNA strands into an organized sandwich structure (L_α^c). McManus et al. [24] reported the coexistence of two lamellar phases in the structure of DNA+DPPC+Ca^{2+} aggregates formed in excess of the lipid phase (DPPC/DNA=8:1 mol/base). They observed the diffraction peak from DNA–DNA correlations at d_{DNA}=5.14 nm in the temperature range corresponding to the DPPC gel phases (~25 °C–40 °C). In the liquid–crystalline phase of DPPC, the peak from DNA–DNA correlations was not observed. These authors supposed that this peak was obscured or masked by the peaks arising from the two lipid phases. Another possible explanation of the absence of a DNA reflection is a high topological disorder of DNA strands placed between lipid bilayers. The absence of DNA reflection in SAX region of diffractograms was also reported [25] in the study of the structure of DOPC–DNA–Mn^{2+} aggregates. These authors supposed that the

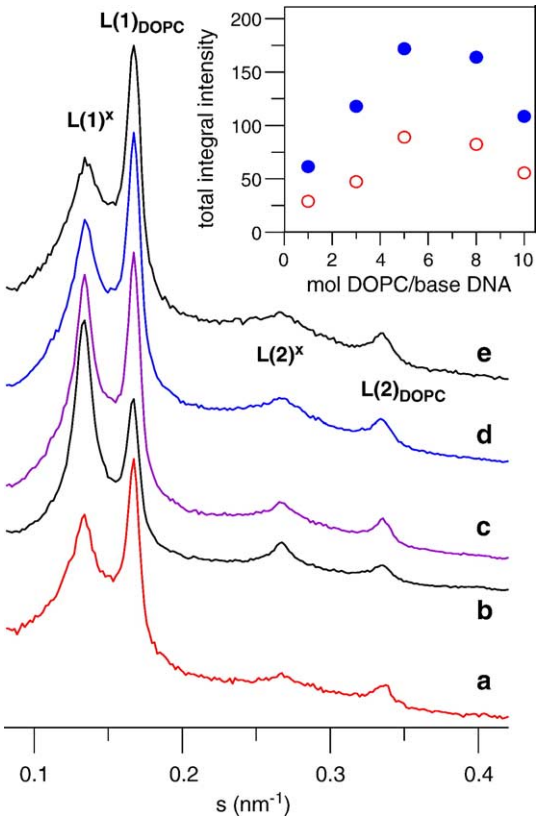

Fig. 9. SAXD patterns of DOPC+DNA+Ca^{2+} aggregates at 20 °C prepared in 20 mM $CaCl_2$ and DOPC/DNA molar ratio: (a) 1:1; (b) 3:1; (c) 5:1; (d) 8:1 and (e) 10:1; inset: the total integral intensities of L^x phase (●) and L_{DOPC} phase (○).

higher mobility of the metal ions does not induce enough constraints to allow the DNA chains to assume a regular packing within the lipid bilayers. Because packing of DNA strands in this phase is unclear, we use abbreviation L^x.

Our analysis of experimental data indicates the coexistence of both phases in one aggregate—we have not observed any macroscopic separation in the sample sediment. We prepared a set of samples with DNA/DOPC = 1:1 base/mol in 20 mM $CaCl_2$, where the mixtures of D_2O/H_2O were used as solvent, with a density that can be tuned between 1 and 1.1 g/cm^3. The density of the aggregate is inside this range, because it floats on top of the most dense and at the bottom of the least dense solvent. We did not observe any macroscopic separation of the sample sediment, even when the specific densities of the H_2O/D_2O mixtures differed by only 4.3 10^{-3} g/cm^3.

We have shown that 10 days incubation of aggregates or heating over a wide temperature range does not induce dramatic changes in the structural organization of aggregates and the structure displays excellent stability. The repeat distances and lipid bilayer fluctuations of both phases reflect changes due to cation concentration, amount of lipid, length of DNA fragments and temperature. The presence of a partially dehydrated phase (L_{DOPC}) in samples prepared in excess of water indicates the coexistence of this phase in osmotic equilibrium with a "polymer stressing solution". It is known that DNA itself can be thought as an osmometer [60,61]. We have found, that with increasing amounts of lipid, the fraction of partially dehydrated DOPC phase (L_{DOPC}) is limited and depends on the portion of DNA in the sample and also on the length of DNA fragments. The obtained stoichiometry of binding of DOPC/DNA ~5:1 mol/base in 20 mM Ca^{2+} is related to the total volume of lipid in the sample, which is distributed into L^x and L_{DOPC} phase. The ratio of the fractions of each phase (X_{DOPC}/X_{Lx} ~0.5) indicates a distribution of DOPC molecules among both phases. It was suggested that the presence of negatively charged DNA between bilayers can induce a partial lateral segregation of cationic surfactants in bilayers to minimize the electrostatic energy of the whole system, i.e., lateral "demixing" in the plane of the bilayers can occur [62–64]. Such a demixing was observed experimentally in 1-palmitoyl-2-oleoyl-*sn*-glycero-3-phosphorylcholine vesicles containing various cationic surfactants and interacting with polyadenylic acid [65]. MacDonald et al. [66] have shown that adding polyelectrolytes to lipid bilayers consisting of mixtures of oppositely charged and zwitterionic lipids produces ^{2}H NMR spectra which are superpositions of two sub-spectra: one corresponding to a polyelectrolyte-bound lipid population, and the other to a polyelectrolyte-free population. Quantitative analysis of the two sub-spectra indicates that the polyelectrolyte-bound population is enriched with oppositely charged lipid, while the polyelectrolyte-free lipid population is correspondingly depleted. These experiments were performed with cationic surfactants which are "anchored" in the lipid bilayer as a result of hydrophobic interactions between the hydrophobic core of lipid bilayers and the alkyl chains of surfactants molecules. The analysis of our data indicates a similar structural organization of DNA–DOPC–cation^{2+} aggregates, despite the higher mobility of divalent cations.

5. Conclusions

Two lamellar phases form in aggregates of DNA with DOPC vesicles in presence of divalent cations (Ca^{2+}, Mg^{2+}). One phase is a condensed lamellar phase with DNA strands intercalated between lipid bilayers. The second lamellar phase consists of pure DOPC bilayers, without any divalent cations and DNA strands, and is partially dehydrated. The fraction of the partially dehydrated phase depends on the portion of DNA in the sample and also on the length of DNA fragments. The coexistence of two phases in one aggregate can be explained by a lateral segregation of DNA and metal cations that minimizes the electrostatic energy of the whole system.

Acknowledgements

This work was supported by the European Community-Research Infrastructure Action under the FP6 "Structuring the European Research Area" Programme (through the Integrated Infrastructure Initiative "Integrating Activity on Synchrotron and Free Electron Laser Science"): RII3-CT-2004-506008 (IA-SFS), HASYLAB project II-02-016; by the JINR project 07-4-1031-99/2008 and by the VEGA grant 1/0123/03 to PB. DU thanks the staff of HASYLAB for his hospitality. PB thanks MB for 44 years of friendship and intellectual stimulation.

References

[1] A.P. Rolland, From genes to gene medicines: recent advances in nonviral gene delivery, Crit. Rev. Ther. Drug Carr. Syst. 15 (1998) 143–198.
[2] I.M. Verma, N. Somia, Gene therapy—Promises, problems and prospects, Nature 389 (1997) 239–242.
[3] P.L. Felgner, G.M. Ringold, Cationic liposome-mediated transfection, Nature 337 (1989) 387–388.
[4] B. Sternberg, F.L. Sorgi, L. Huang, New structures in complex formation between DNA and cationic liposomes visualized by freeze-fracture electron microscopy, FEBS Lett. 356 (1994) 361–366.
[5] I. Koltover, T. Salditt, J.O. Radler, C.R. Safinya, An inverted hexagonal phase of cationic liposome–DNA complexes related to DNA release and delivery, Science 281 (1998) 78–81.
[6] T. Salditt, I. Koltover, J.O. Radler, C.R. Safinya, Two-dimensional smectic ordering of linear DNA chains in self-assembled DNA–cationic liposome mixtures, Phys. Rev. Lett. 79 (1997) 2582–2585.
[7] P.L. Felgner, T.R. Gadek, M. Holm, R. Roman, H.W. Chan, M. Wenz, J.P. Northrop, G.M. Ringold, M. Danielsen, Lipofection: a highly efficient, lipid-mediated DNA-transfection procedure, Proc. Natl. Acad. Sci. U. S. A. 84 (1987) 7413–7417.

[8] A.D. Miller, Cationic liposomes for gene therapy, Angew. Chem., Int. Ed. 37 (1998) 1769–1785.
[9] A.J. Kirby, P. Camilleri, J.B.F.N. Engberts, M.C. Feiters, R.J.M. Nolte, O. Soderman, M. Bergsma, P.C. Bell, M.L. Fielden, C.L.G. Rodriguez, P. Guedat, A. Kremer, C. McGregor, C. Perrin, G. Ronsin, M.C.P. van Eijk, Gemini surfactants: new synthetic vectors for gene transfection, Angew. Chem., Int. Ed. 42 (2003) 1448–1457.
[10] V.G. Budker, Y.A. Kazatchkov, L.P. Naumova, Polynucleotides adsorb on mitochondrial and model lipid membranes in the presence of bivalent cations, FEBS Lett. 95 (1978) 143–146.
[11] L. Vojčíková, P. Balgavý, Interaction of DNA with dipalmitoylphosphatidylcholine model membranes: A microcalorimetric study, Stud. Biophys. 125 (1988) 5–10.
[12] Y.S. Tarahovsky, A.V. Khusainova, A.V. Gorelov, T.I. Nicolaeva, A.A. Deev, A.K. Dawson, G.R. Ivanitsky, DNA initiates polymorphic structural transitions in lecithin, FEBS Lett. 390 (1996) 133–136.
[13] D. Uhríková, G. Rapp, P. Balgavý, Condensation of DNA and phosphatidylcholine bilayers induced by Mg(II) ions—A synchrotron X-ray diffraction study, in: M. Melník, A. Sirota (Eds.), Challenges for Coordination Chemistry in the new Century, vol. 5, Slovak Technical Univ. Press, Bratislava, 2001, pp. 219–224.
[14] Y. Inoko, T. Yamaguchi, K. Furuya, T. Mitsui, Effects of cations on dipalmitoyl phosphatidylcholine/cholesterol/water systems, Biochim. Biophys. Acta 413 (1975) 24–32.
[15] S.A. Tatulian, V.I. Gordeliy, A.E. Sokolova, A.G. Syrykh, A neutron diffraction study of the influence of ions on phospholipid membrane interactions, Biochim. Biophys. Acta 1070 (1991) 143–151.
[16] K. Akashi, H. Miyata, H. Itoh, K. Kinosita, Formation of giant liposomes promoted by divalent cations: critical role of electrostatic repulsion, Biophys. J. 74 (1998) 2973–2982.
[17] V.G. Budker, A.A. Godovikov, L.P. Naumova, I.A. Slepneva, Interaction of polynucleotides with natural and model membranes, Nucleic Acid Res. 8 (1980) 2499–2515.
[18] L. Vojčíková, E. Švajdlenka, P. Balgavý, Spin label and microcalorimetric studies of the interaction of DNA with unilamellar phosphatidylcholine liposomes, Gen. Physiol. Biophys. 8 (1989) 399–406.
[19] L. Vojčíková, Studies of structural changes in aggregates of DNA with model phosphatidylcholine membranes, Ph.D. Thesis, Faculty of Sciences of the P.J. Šafárik University and Faculty of Mathematics and Physics of the J.A. Comenius University, Bratislava, 1990.
[20] R.S. Khusainova, A.A. Khusainov, V.I. Popov, K.A. Dawson, G.R. Ivanitsky, Detection of aggregate states of DNA–Ca^{2+}–dipalmitoylphosphatidylcholine complexes using microcalorimetric studies, Dokl. Akad. Nauk 367 (1999) 416–419.
[21] Y.S. Tarahovsky, A.A. Deev, I.S. Masulis, G.R. Ivanitsky, Structural organization and phase behavior of DNA–calcium–dipalmitoylphosphatidylcholine complex, Biochemistry (Moscow) 63 (1998) 1126–1131.
[22] R.S. Khusainova, K.A. Dawson, I. Rochev, A.V. Gorelov, G.R. Ivanitsky, Structural changes in DNA–Ca^{2+}–dipalmitoylphosphatidylcholine complexes during changes in the molar ratio of nucleotide/lipid. Microcalorimetric study, Dokl. Akad. Nauk 367 (1999) 553–556.
[23] J. McManus, J.O. Radler, A.K. Dawson, Does calcium turn a zwitterionic lipid cationic? J. Phys. Chem., B 107 (2003) 9869–9875.
[24] J. McManus, J.O. Radler, K.A. Dawson, Phase behaviour of DPPC in a DNA–calcium–zwitterionic lipid complex studied by small angle X-ray scattering, Langmuir 19 (2003) 9630–9637.
[25] O. Francescangeli, V. Stanic, L. Gobbi, P. Bruni, M. Iacussi, G. Tosi, S. Bernstorff, Structure of self-assembled liposomeDNAmetal complexes, Phys. Rev., E 67 (2003) 011904-1–011904-11.
[26] I. Koltover, K. Wagner, C.R. Safinya, DNA condensation in two dimensions, Proc. Natl. Acad. Sci. U. S. A. 97 (2000) 14046–14051.
[27] D.V. Kovalenko, R.A. Shafei, I.A. Zelenina, M.L. Semenova, O.V. Samuilova, R.I. Zhdanov, Metallonucleoliposome complexes as a vehicle for gene delivery to mouse skeletal muscles in vivo, Genetika 32 (1996) 1299–1301.
[28] R.I. Zhdanov, O.A. Buneeva, O.V. Podobed, N.G. Kutsenko, T.A. Tsvetkova, T.P. Lavrenova, Transfer of the functional genes into eucaryotic cells by neutral phospholipid liposomes, Vopr. Med. Him. 43 (1997) 212–216.
[29] R.I. Zhdanov, O.V. Podobed, N.G. Kutsenko, O.A. Buneeva, T.A. Tsvetkova, S.O. Gur'ev, T.P. Lavrenova, G.A. Serebrennikova, I.D. Konstantinova, M.A. Maslov, New cationic liposomes for transfecting eukaryotic cells, Dokl. Akad. Nauk 362 (1998) 557–560.
[30] J. Sambrook, E.F. Fritsch, T. Maniatis, Gel Electrophoresis of DNA, Molecular Cloning: A Laboratory Manual, Cold Spring Harbor Laboratory Press, New York, 1989.
[31] P. Doty, B.B. McGill, S.A. Rice, The properties of sonic fragments of deoxyribose nucleic acid, Proc. Natl. Acad. Sci U. S. A. 44 (1958) 432–438.
[32] T.C. Huang, H. Toraya, T.N. Blanton, Y. Wu, X-ray-powder diffraction analysis of silver behenate, a possible low-angle diffraction standard, J. Appl. Crystallogr. 26 (1993) 180–184.
[33] D. Chapman, The polymorphism of glycerides, Chem. Rev. 62 (1962) 433–453.
[34] M. Kellens, W. Meeussen, H. Reynaers, Crystallization and phase-transition studies of tripalmitin, Chem. Phys. Lipids 55 (1990) 163–178.
[35] C. Boulin, R. Kempf, M.H.J. Koch, S.M. McLaughlin, Data appraisal, evaluation and display for synchrotron radiation experiments—Hardware and software, Nucl. Instrum. Methods Phys. Res., Sect. A, Accel. Spectrom. Detect. Assoc. Equip. 249 (1986) 399.
[36] F. Artzner, R. Zantl, G. Rapp, J.O. Radler, Observation of a rectangular columnar phase in condensed lamellar cationic lipid–DNA complexes, Phys. Rev. Lett. 81 (1998) 5015.
[37] J.F. Nagle, S. Tristram-Nagle, Structure of lipid bilayers, Biochim. Biophys. Acta 1469 (2000) 159–195.
[38] K. Gawrisch, W. Richter, A. Möpps, P. Balgavý, K. Arnold, G. Klose, The influence of water concentration on the structure of egg yolk phospholipid/water dispersions, Stud. Biophys. 108 (1985) 5–16.
[39] S. Tristram-Nagle, H.I. Petrache, J.F. Nagle, Structure and interaction of fully hydrated dioleoylphosphatidylcholine bilayers, Biophys. J. 75 (1998) 917–925.
[40] D. Uhríková, A.V. Khusainova, M. Hanulová, A. Islamov, S.S. Funari, P. Balgavý, SANS and SAXS study of DNA+DOPC+Ca^{2+} aggregates, XII International Conference on Selected Problems of Modern Physics, JINR Dubna, Russia, June 8–11, 2003, p. 216 (Book of abstracts).
[41] N. Kučerka, D. Uhríková, J. Teixeira, P. Balgavý, Lipid bilayer thickness in extruded liposomes prepared from 1,2-diacylphosphatidylcholines with monounsaturated acyl chains: a small-angle neutron scattering study, Acta Fac. Pharm., Univ. Comen. 50 (2003) 78–89.
[42] M.J. Ruocco, G.G. Shipley, Characterization of the sub-transition of hydrated dipalmitoylphosphatidylcholine bilayers—Kinetic, hydration and structural study, Biochim. Biophys. Acta 691 (1982) 309–320.
[43] M.J. Janiak, B.M. Small, G.G. Shipley, Nature of thermal pretransition of synthetic phospholipids—Dimyristoyllecithin and dipalmitoyllecithin, Biochemistry (USA) 15 (1976) 4575–4580.
[44] H.I. Petrache, S. Tristram-Nagle, J.F. Nagle, Fluid phase structure of EPC and DMPC bilayers, Chem. Phys. Lipids 95 (1998) 83–94.
[45] R. Zhang, S. Tristram-Nagle, W. Sun, R.L. Headrick, T.C. Irving, R.M. Suter, J.F. Nagle, Small-angle X-ray scattering from lipid bilayers is well described by modified Caille theory but not by paracrystalline theory, Biophys. J. 70 (1996) 349–357.
[46] A.C. Cowley, N.L. Fuller, R.P. Rand, V.A. Parsegian, Measurement of repulsive forces between charged phospholipid bilayers, Biochemistry (USA) 17 (1978) 3163–3168.
[47] R. Zhdanov, V. Kuvichkin, Membrane phospholipids act as DNA/RNA receptors during formation of specific DNA–nuclear membrane contacts and gene expression: a hypothesis based on the study of interaction between phospholipid vesicles and DNA or

polynucleotides, in: J.A. Gustafson, K.W.A. Wirtz (Eds.), New Developments in Lipid–protein Interactions and Receptor Function, Plenum, New York, 1993, pp. 249–262.
[48] D. Uhríková, G. Rapp, P. Balgavý, Condensed lamellar phase in ternary DNA-DLPC-cationic gemini surfactant system: a small-angle synchrotron X-ray diffraction study, Bioelectrochemistry 58 (2002) 87–95.
[49] J.C. Shepherd, G. Buldt, Zwitterionic dipoles as a dielectric probe for investigating head group mobility in phospholipid membranes, Biochim. Biophys. Acta 514 (1978) 83–94.
[50] Y. Izumitani, Cation dipole interaction in the lamellar structure of DPPC bilayers, J. Colloid Int. Sci. 166 (1994) 143–159.
[51] E.G. Finer, Interpretation of ^{2}H NMR of the hydration of macromolecules, J. Chem. Soc. Faraday Trans. 2 (1973) 1590–1600.
[52] K. Gawrisch, K. Arnold, T. Gottwald, G. Klose, F. Volke, ^{2}H NMR studies of the phosphate–water interaction in dipalmitoylphosphatidylcholine–water systems, Stud. Biophys. 74 (1978) 1–10.
[53] T.J. McIntosh, A.D. Magid, Phospholipid hydration, in: G. Cevc (Ed.), Phospholipid Handbook, Marcel Dekker Inc., New York, 1993, pp. 553–578.
[54] K. Hayakawa, J.P. Santerre, J.C.T. Kwak, The binding of cationic surfactants by DNA, Biophys. Chem. 17 (1983) 175–181.
[55] M. Hammel, D. Uhríková, P. Balgavý, Partition of local anesthetic heptacaine homologs between phospholipid bilayer in liposomes and aqueous phase estimated by UV spectrophotometry, Pharmazie 57 (2002) 499.
[56] D.P. Kharakoz, R.S. Khusainova, A.V. Gorelov, K.A. Dawson, Stoichiometry of dipalmitoylphosphatidylcholine–DNA interaction in the presence of Ca^{2+}: a temperature-scanning ultrasonic study, FEBS Lett. 446 (1999) 27–29.
[57] J.O. Radler, I. Koltover, T. Salditt, C.R. Safinya, Structure of DNA–cationic liposome complexes: DNA intercalation in multilamellar membranes in distinct interhelical packing regimes, Science 275 (1997) 810–814.
[58] I. Koltover, T. Salditt, C.R. Safinya, Phase diagram, stability, and overcharging of lamellar cationic lipid–DNA self-assembled complexes, Biophys. J. 77 (1999) 915–924.
[59] R. Zantl, F. Artzner, G. Rapp, J.O. Radler, Thermotropic structural changes of saturated-cationic–lipid–DNA complexes, Europhys. Lett. 45 (1999) 90–96.
[60] V.A. Parsegian, R.P. Rand, N.L. Fuller, D.C. Rau, Osmotic-stress for the direct measurement of intermolecular forces, Methods Enzymol. 127 (1986) 400–416.
[61] V.A. Parsegian, R.P. Rand, D.C. Rau, Macromolecules and water: probing with osmotic stress, Methods Enzymol. 259 (1995) 43–93.
[62] R. Bruinsma, J. Mashl, Long-range electrostatic interaction in DNA–cationic lipid complexes, Europhys. Lett. 41 (1998) 165–170.
[63] R. Bruinsma, Electrostatics of DNA cationic lipid complexes: isoelectric instability, Eur. Phys. J., B Cond. Matter Phys. 4 (1998) 75–88.
[64] D. Harries, S. May, W.M. Gelbart, A. Ben Shaul, Structure, stability, and thermodynamics of lamellar DNA–lipid complexes, Biophys. J. 75 (1998) 159–173.
[65] P. Mitrakos, P.M. MacDonald, DNA induced lateral segregation of cationic amphiphiles in lipid bilayer membranes as detected via ^{2}H NMR, Biochemistry (USA) 35 (1996) 16714–16722.
[66] P.M. MacDonald, K.J. Crowell, C.M. Franzin, P. Mitrakos, D. Semchyschyn, ^{2}H NMR and polyelectrolyte-induced domains in lipid bilayers, Solid State Nucl. Magn. Reson. 16 (2000) 21–36.